PROCEEDINGS OF THE ROYAL SOCIETY B

Proc. R. Soc. B (2010) **277**, 3265–3274
doi:10.1098/rspb.2010.0735
Published online 10 June 2010

Growth-induced mass flows in fungal networks

Luke L. M. Heaton[1,2], Eduardo López[2,3], Philip K. Maini[3,4,5], Mark D. Fricker[3,6] and Nick S. Jones[2,3,5,*]

[1]*LSI DTC, Wolfson Building, University of Oxford, Parks Road, Oxford OX1 3QD, UK*
[2]*Physics Department, Clarendon Laboratory, University of Oxford, Parks Road, Oxford OX1 3PU, UK*
[3]*CABDyN Complexity Centre, Saïd Business School, University of Oxford, Park End Street, Oxford OX1 1HP, UK*
[4]*Centre for Mathematical Biology, Mathematical Institute, University of Oxford, 24-29 St Giles', Oxford OX1 3LB, UK*
[5]*Oxford Centre for Integrative Systems Biology, Department of Biochemistry, University of Oxford, South Parks Road, Oxford OX1 3QU, UK*
[6]*Department of Plant Sciences, University of Oxford, South Parks Road, Oxford OX1 3RB, UK*

Cord-forming fungi form extensive networks that continuously adapt to maintain an efficient transport system. As osmotically driven water uptake is often distal from the tips, and aqueous fluids are incompressible, we propose that growth induces mass flows across the mycelium, whether or not there are intrahyphal concentration gradients. We imaged the temporal evolution of networks formed by *Phanerochaete velutina*, and at each stage calculated the unique set of currents that account for the observed changes in cord volume, while minimizing the work required to overcome viscous drag. Predicted speeds were in reasonable agreement with experimental data, and the pressure gradients needed to produce these flows are small. Furthermore, cords that were predicted to carry fast-moving or large currents were significantly more likely to increase in size than cords with slow-moving or small currents. The incompressibility of the fluids within fungi means there is a rapid global response to local fluid movements. Hence velocity of fluid flow is a local signal that conveys quasi-global information about the role of a cord within the mycelium. We suggest that fluid incompressibility and the coupling of growth and mass flow are critical physical features that enable the development of efficient, adaptive biological transport networks.

Keywords: mycelial modelling; nutrient translocation; complex networks

1. INTRODUCTION

Multicellular organisms have evolved sophisticated systems to supply individual cells with the resources necessary for survival. Plants circulate nutrients through the xylem and phloem, driving mass flows in the xylem by transpiration from the leaves. They also actively maintain osmotic gradients along the phloem, inducing a flow of sap from sources, where water is drawn from the surrounding tissue into the sieve-tubes of the phloem, to sinks, where water leaves the phloem (Nobel 1991; Nelson 2003). Animals use hearts or contractile regions to circulate blood through hierarchical, fractal-like vascular systems (Sherman 1981; Savage *et al.* 2008). In contrast, transport through fungal mycelial networks is poorly understood.

Foraging fungal mycelia continuously remodel their morphology, and as a transport network the mycelium must adapt to changing local environmental conditions and patchy resource availability (Jennings 1987; Cairney 1992; Gow & Gadd 1995; Boddy 1999; Falconer *et al.* 2005, 2007; Bebber *et al.* 2007; Fricker *et al.* 2007). Hyphae grow by tip extension and then branch subapically to form a diffuse tree-like mycelium (Howard 1981; Gooday 1995; Heath & Steinberg 1999; Money 1997, 2008; Steinberg 2006). As the colony continues to grow, hyphal fusions or anastomoses occur, producing a more reticulate, net-like structure. In cord-forming fungi, hyphal aggregates subsequently develop and undergo limited differentiation to yield specialized high-conductivity channels that are often well insulated from the environment (Jennings 1987; Rayner *et al.* 1991; Cairney 1992). These 'cords' may thicken or thin over time, and they contain numerous rigid, hollow vessel hyphae with very few septal pores (Eamus *et al.* 1985). Other regions of the mycelium regress, probably by autophagy, to recycle redundant material to support new growth (Olsson 2001; Falconer *et al.* 2005, 2007; Fricker *et al.* 2007).

While direct uptake and intra-hyphal nutrient diffusion may be sufficient to sustain short-range local growth when resources are abundant (Olsson 2001), long-distance translocation is required to deliver nutrients at a sufficient rate to growing tips, particularly in non-resource restricted fungi that are too large to distribute nutrients through diffusion alone (Eamus & Jennings 1984; Clipson *et al.* 1987; Wells & Boddy 1995; Wells *et al.* 1995; Boswell *et al.* 2002, 2003*a*,*b*, 2007). Remarkably little is known about the mechanism(s) underpinning such long-distance nutrient translocation, or the

* Author for correspondence (nick.jones@physics.ox.ac.uk).

Electronic supplementary material is available at http://dx.doi.org/10.1098/rspb.2010.0735 or via http://rspb.royalsocietypublishing.org.

Received 6 April 2010
Accepted 18 May 2010

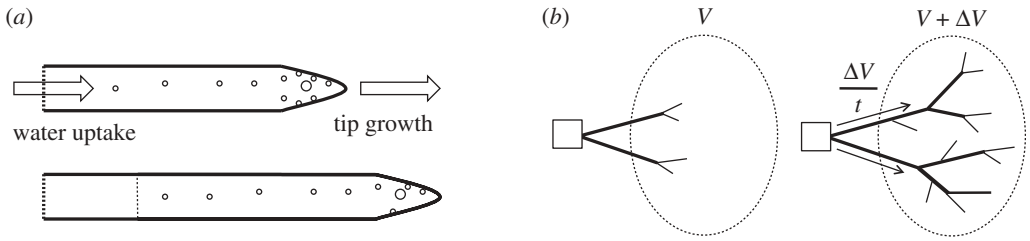

Figure 1. Physical principles of growth-induced mass flow. (*a*) Turgor pressure is induced by an osmotic gradient at the site of water uptake. Vesicles (circles) move towards the tip faster than it recedes, while the cytosol behind the growing tip moves forward at the rate of tip growth (Lew 2005). The conservation of volume dictates that as the tip expands, fluid flows towards the tips from the site of water uptake. This mass flow demonstrates the presence of a pressure gradient. (*b*) Suppose that a fungus grows out of an inoculum (square) and into a region (oval). Some of the material that becomes part of the fungi may come from within the oval region. The rest of the material must have travelled along the cords (edges) that cross the region's boundary. If the volume of fungi within the region increases by ΔV over a period of time t, and none of the material is drawn from within the region, it follows that the net current flowing into the region is $\Delta V/t$. Furthermore, if the total cross-sectional area of the boundary crossing cords is a, the mean velocity of flow will be $\Delta V/at$.

quantitative contribution of different potential transport pathways, such as cytoplasmic streaming, vesicle transport or mass flow to net fluxes and overall nutrient dynamics (Jennings 1987; Cairney 1992; Fricker *et al.* 2007).

We suggest that regardless of intra-hyphal concentration gradients, mass flow only takes place when water is able to exit the translocation pathway through either localized exudation (e.g. *Serpula lacrymans*), evaporation or by moving into a region of new growth. In this paper, we quantify the last of these phenomena, which we have termed growth-induced mass flow. By way of physical analogy, consider a rigid tube filled with salty water that is blocked at one end by a semi-permeable membrane, while the other end is blocked by a thin rubber cap. If this apparatus is submerged in water, the osmotic gradient across the semi-permeable membrane will induce turgor pressure and the pressure within the tube will force the rubber cap to bulge outwards. As aqueous fluids are essentially incompressible, the column of fluid within the tube can only move forward at the same rate as the rubber cap, and this movement indicates the presence of a pressure gradient (figure 1*a*).

Injected oil droplets in individual hyphae of *Neurospora* provide evidence for this kind of growth-coupled mass flow, as the average rate of movement (approx. $0.5\ \mu m\ s^{-1}$) matches the rate of tip extension (Lew 2005). Such movement would be consistent with mass flow driven by the continuous subapical water influx required to sustain volume increases at the tip during growth. Taken together, these lines of evidence suggest growth-coupled mass flow may have a significant role in water and nutrient translocation in larger mycelial systems.

To quantify the scale of growth-induced mass flow we developed two models, the 'uniform model' and the 'time-lapse model', and applied these models to measured examples of mycelial growth. To obtain a sample of fungal networks we allowed *Phanerochaete velutina* to grow over experimental microcosms for a four week period, taking photographs every three days. An image analysis program was then used to convert the sequence of photographs into a sequence of networks, composed of cords of measured length and volume. Given the measured volumes and changes in volume, we used these models to calculate a current for each edge. The currents calculated by the uniform model reflect the topology of the network. The time-lapse model produces an estimate for the minimum flow of material that is consistent with the measured changes in volume, under the assumption that the inoculum is the sole source of water and nutrients.

We found that the cords with higher currents or higher speeds of mass flow were more likely to increase in thickness than the other cords (see §4). This suggests that our model is correctly identifying the high current cords, since thickening the high current cords is an efficient way to remodel a fungal network. This follows because increasing the thickness and conductance of any cord will reduce the cost of overcoming viscous drag, but it is much more efficient to thicken cords that carry large currents than those with small currents.

2. MODEL DEVELOPMENT

By definition a network is a collection of nodes together with the edges that connect those nodes. A node that is connected to a single edge is called a 'tip', and we refer to all other edges as 'cords'. By this definition a cord is a cylindrical, linear structure, while any branching fungal form is described as a network of cords and tips. We use letters such as i and j to index nodes, and pairs of letters ij index the edge between nodes i and j. In this paper we describe two models that can be unfolded over a given network: the 'uniform model' and the 'time-lapse model'. Details are supplied in later sections, and a preview can be gained by a glance at figure 2 or the electronic supplementary material, fig. S1. Both models take as their inputs experimentally determined networks extracted from images; how these image data are used to calculate currents differs between the two cases. Furthermore, both models have been defined for water uptake at a single location (the inoculum), but could be adapted for growth involving more than one source of nutrients and water.

The uniform model uses only a small amount of information from a single imaged network: it discards all detail about the thickness of cords (but not their lengths) and supposes they are of uniform thickness. It calculates currents by supposing that all tips grow at the same rate. Given any network, the output of the uniform model is

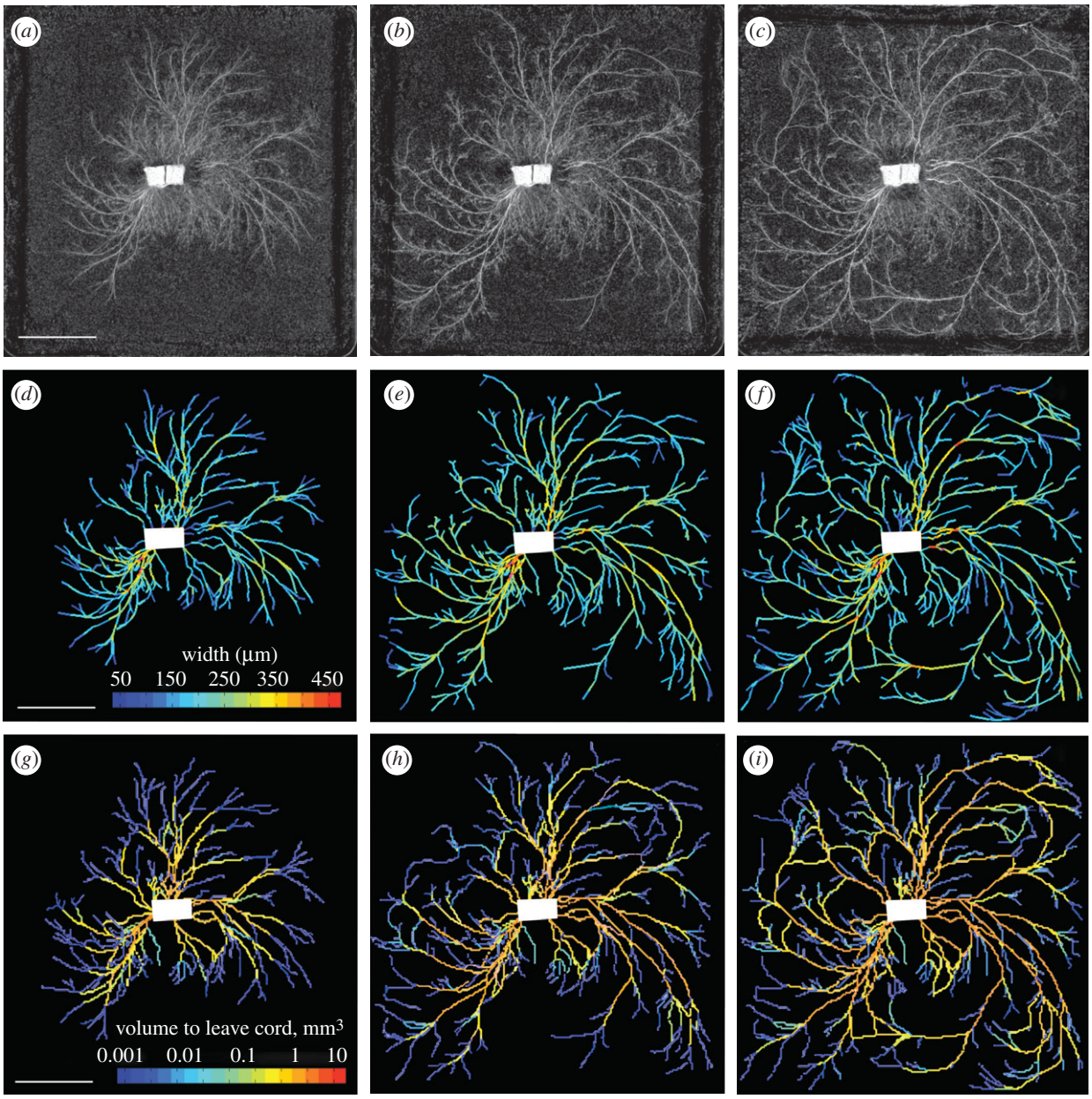

Figure 2. Network development and predicted currents in *P. velutina*. (*a–c*) Network development in *P. velutina* after 19 days, 25 days and 32 days. The image intensity of cords was used to estimate their thickness, enabling the production of the weighted, digitized networks (*d–f*). These are colour-coded to show the estimated thicknesses of all sections of all edges. Images (*g–i*) are colour-coded according to the total volume that has passed through each cord, as calculated by using the time-lapse model (scale bars, 50 mm).

a 'current' for each cord. This quantity reflects the topological location of the cords, and the currents predicted by the uniform model reflect the number of tips 'downstream' from each of the given cords (see the electronic supplementary material, §S1 and fig. S1*a*). We found that under the uniform model, cords with a large current tend to be thicker than cords with a small current.

While the uniform model calculates currents by assuming that all tips grow at the same rate, the time-lapse model uses observed changes in volume between successive pairs of aligned networks. We effectively derive a minimal set of currents that are consistent with the measured growth. A key principle behind the time-lapse model is that if an object (e.g. a thickening cord) is composed of incompressible material, the rate of increase in the volume of that object must equal the rate of flow into that object minus the rate of flow out of that object. Growth requires the flow of materials, and the time-lapse model was designed to quantify the extent to which changes in volume generate mass flows through the supporting mycelial network. The currents we will calculate represent a minimal total flux, found by calculating the unique set of currents that account for the observed changes in cord volume, while minimizing the work required to overcome viscous drag.

(a) *Pressure gradients, hydraulic conductance, current and velocity*

The relationships between pressure gradients, hydraulic conductance, current and velocity are fundamental to understanding fluid flows in plants and fungi. We note, however, that there is no close analogy between flows in open-ended plant vessels that are permeable along their

lengths and close-ended fungal vessels with hydrophobic coatings. In plants, concentration gradients draw water from the surrounding tissue into, and out of, the xylem and phloem all along their lengths. By contrast, fungal cords have hydrophobic coatings, and we suppose that such cords do not directly draw fluid from their surrounding environment (in our model, water uptake only occurs at the inoculum). In plants one expects flow between two points to be explained by a chemical potential difference. Similarly, in fungi there is a chemical potential difference between the environment and the hyphae responsible for water and nutrient uptake, and the fungus must do work to maintain such osmotic gradients (Amir *et al.* 1995*a*,*b*; Bancal & Soltani 2002; Lew *et al.* 2004). However, flows between two points *within* the fungus need not be caused by chemical potential differences between those points. The physical effects of growth, turgor pressure and fluid incompressibility may suffice to create flows across the mycelium.

Our models require no commitments concerning the mechanisms of fungal growth: fluid incompressibility means that volume is conserved regardless of the mechanisms driving fungal fluid flows. We make the simplifying assumption that the inoculum is the sole source of extra fluid, and the presence of this fluid enables the volume change we observe in the growing fungus. Of the possible set of current flows consistent with the observed changes in volume, we parsimoniously identify the unique flows which minimize energy losses to resistance. Since the fluid flows within fungi are laminar (see the electronic supplementary information, §S3), it is appropriate to apply the Hagen–Poiseuille equation, which accurately describes the laminar flow of incompressible fluids along an insulated tube.

By definition (and by analogy with Ohm's law), the current in a cord must be equal to the pressure drop times the conductance (Eamus *et al.* 1985; Nobel 1991). The size of the conducting vessels within a cord does not vary significantly with the size of the cord. We are therefore motivated to assume that all cords contain tubes of some fixed radius. We also assume that the number of tubes per unit of cross-sectional area is constant throughout the network. The Hagen–Poiseuille equation tells us that the total current f through a cord composed of n tubes will satisfy the equation

$$f = \Delta P C = \Delta P \frac{n\pi r^4}{8\eta l} = \sigma \Delta P A, \tag{2.1}$$

where ΔP is the pressure drop between the ends of the cord, C the hydraulic conductance of cord, r the radius of the tubes, η the dynamic viscosity of the fluid, l the length of the cord, A the cross-sectional area of the cord and σ a constant of proportionality. The conductance of a cord is proportional to the number of tubes it contains, and if we assume a constant density of tubes, conductance is proportional to cross-sectional area.

(b) *Modelling fluid flows: the uniform model*

The 'uniform model' described in this section takes as its input an empirically observed fungal network, where each cylindrical cord in the network has a measured length. We have called it the uniform model because we assume uniform conductance (cross-sectional area) throughout the network, and assume a unit current outflow at every tip.

The rules governing the uniform model are as follows:

— We assume unit growth at every tip, so there is a unit current flowing towards each tip.
— The net current flowing away from the inoculum is equal to the total number of tips. In other words, water uptake occurs at the inoculum, and the rate of water uptake equals the total rate of growth.
— All cords have the same resistance per unit length. In other words, the conductance of each cord is inversely proportional to its length.

Current effectively enters the network at the inoculum (source) and exits at the tips (sinks). Elsewhere the currents of an incompressible fluid must obey Kirchhoff's law, which states that the total current flowing into a point must equal the total current flowing out. In other words, the net current must be zero. It follows that where q_i is the net current flowing out of node i,

$$q_i = \begin{cases} -1 & \text{if node } i \text{ is a tip,} \\ m & \text{if node } i \text{ is the inoculum} \\ & \quad \text{(where } m \text{ is the number of tips),} \\ 0 & \text{otherwise.} \end{cases} \tag{2.2}$$

Note that the net current at the inoculum is positive, because the flow is directed away from the inoculum. Equation (2.1) tells us that the current in a cord is equal to the pressure drop times the conductance. We can use this fact to sum the currents that flow in or out of node i, so we have

$$\sum_j (p_i - p_j) C_{ij} = q_i, \tag{2.3}$$

where p_i is the pressure at node i and C_{ij} is the conductance of the cord between nodes i and j. In the uniform model,

$$C_{ij} = \begin{cases} 0 & \text{if nodes } i \text{ and } j \text{ are not directly connected,} \\ \dfrac{1}{l_{ij}} & \text{if there is a cord } ij \text{ of length } l_{ij}. \end{cases} \tag{2.4}$$

Given the conductance of each cord and the net current flowing out of each node, we can uniquely determine the pressure difference between any pair of nodes (see the electronic supplementary material, §S2, or Grimmett & Kesten 1984; López *et al.* 2005). Furthermore, by equation (2.1) we can uniquely determine the currents in the network.

(c) *Modelling currents induced by changes in volume: the time-lapse model*

Each experiment yielded a sequence of 11 digitized networks. Unlike the uniform model, the time-lapse model does not assume that the tips are growing at constant rate. Instead, we calculate currents by looking at how each network changes in the next time step. The networks in each sequence must be aligned, and all nodes are considered to be present at all times (so some nodes in a network may not be connected to any edges/cords). We know the time-lapse t between the earlier and later networks, and each cord has a measured length l_{ij}, a volume in the earlier network u_{ij} (though this volume may equal zero), a cross-sectional area in the earlier network $a_{ij} = u_{ij}/l_{ij}$ and a volume in the later network v_{ij}.

To calculate the currents we must know the relative conductances of the cords, and the net current at each node (note that since edges can thicken or narrow they can become sinks and sources like the tips and inoculum). By equation (2.1) the conductance of cords is proportional to their cross-sectional area. Where σ is an arbitrary constant of proportionality and δ is small compared with the cross-sectional areas of the cords, the conductance C_{ij} of cord ij is defined to be

$$C_{ij} = \begin{cases} 0 & \text{if nodes } i \text{ and } j \text{ are not connected,} \\ \dfrac{\sigma a_{ij}}{l_{ij}} & \text{if } i \text{ and } j \text{ are connected in the earlier network,} \\ \dfrac{\sigma \delta}{l_{ij}} & \text{if } i \text{ and } j \text{ are only connected in the later network.} \end{cases} \tag{2.5}$$

In the uniform model the inoculum is the source and each tip is a sink. As noted, in the case where the volume of cords changes over time, thickening cords are sinks, while thinning cords and the inoculum are sources. Now, the volume of cord ij changes from u_{ij} to v_{ij} over a period of time t. Therefore, the current flowing into ij must be $(v_{ij} - u_{ij})/t$ greater than the current flowing out of ij. As a simplifying assumption, we put half of edge ij's demand for current (sink) at node i, and half at node j. In other words, we suppose that the current flowing into node i is $(v_{ij} - u_{ij})/2t$ greater than the current flowing out of node i, and likewise for node j (see equation (2.6)).

In both the uniform model and the time-lapse model the conservation of volume leads us to suppose that the rate of water uptake equals the total rate of growth. Hence the net current at the inoculum must be such that the total net current is zero. There is one final consideration behind the definition of the net currents in the time-lapse model. To make an unbiased analysis of the relationship between current and changes in cross-sectional area, we calculate the current induced in cord $\alpha\beta$ by the changes in volumes of the all the cords excluding cord $\alpha\beta$ itself. For these reasons, when we are calculating the growth-induced current through the cord $\alpha\beta$, the net current flowing out of node i is defined to be

$$q_i = \begin{cases} -\sum\limits_{j \neq i} q_j & \text{if node } i \text{ is the inoculum,} \\ \sum\limits_{ij \neq \alpha\beta} \dfrac{u_{ij} - v_{ij}}{2t} & \text{otherwise.} \end{cases} \tag{2.6}$$

Note that the first sum is over the set of all nodes, while the second sum is over the set of all the cords ij directly connected to node i. As in the uniform model, we can use the conductance of each cord and the net current flowing out of each node to uniquely determine the pressure difference between any pair of nodes (see the electronic supplementary material, §S2 for details on this calculation and a discussion of the model parameters). Given the pressure drop between the nodes, we can use equation (2.1) to uniquely determine the current in each cord. The currents that emerge from this calculation only depend on the empirically determined pair of networks, while the velocities and pressure gradients scale with the model parameters.

3. MATERIAL AND METHODS

(a) *Experimental microcosms*

Cultures of *P. velutina* (DC.) Parmasto were maintained in the Department of Plant Sciences, University of Oxford. The fungus was grown on 2 per cent malt agar (2% no. 3 agar, 2% malt extract; Oxoid, Cambridge, UK) at 22 $\pm$ 1°C in darkness in a temperature-controlled incubator. To create wood inoculae, 1 cm^3 autoclaved beech (*Fagus sylvatica*) blocks (Bagley Wood sawmill, Kennington, UK) were placed on top of *P. velutina* mycelium in the agar culture plates and incubated at 22°C, to allow penetration of the blocks by hyphae. Inoculated wood blocks were placed on a compressed bed of 33 per cent sterile white sand, 50 per cent sterile black sand, and 17 per cent water by weight in a 24-cm square culture dish. Two inoculated blocks were placed side-by-side in the centre of each dish and allowed to grow at 21 $\pm$ 0.5°C in the dark.

(b) *Producing digital networks from the experimental microcosms*

The growing mycelium was photographed every three days, and the sequence of images was manually marked to record the location of nodes or junctions, as well as the presence or absence of edges. The cords were not sufficiently well resolved to make direct measurements of their diameter from the digitized images. However, the reflected intensity, averaged over a small user-defined kernel at either end of the cord, correlated well with microscope-based measurements of cord thickness. The observed relationship between image intensity and thickness was therefore used to estimate cord thickness across the mycelium (linear regression, $r^2 = 0.77$, d.f. = 195, $p < 0.0001$). This calibration was used to estimate the width of cords, while the volume of the mycelium was calculated by assuming that the cords were cylindrical (Jarrett *et al.* 2006; Bebber *et al.* 2007; Fricker *et al.* 2007, 2008).

Three duplicate experiments, photographed over 36 days, were used to generate the results discussed in this paper. In each case the inoculum and resource units were represented as a single node, as the internal mycelial organization was not visible. Estimates for the diameter of cords range from 48 to 480 μm, although fine hyphae and cords smaller than 100 μm are likely to be missing from the digitized network.

4. RESULTS

The total volume of the networks increased in an approximately linear fashion, so the proportional growth dropped significantly over time. The mean rate of increase over the first 21 days was 0.61 $mm^3 h^{-1}$ in the first experiment, 0.51 $mm^3 h^{-1}$ in the second experiment and 1.14 $mm^3 h^{-1}$ in the third experiment. The total number of nodes and cords also increased in an approximately linear fashion, with around two cords and two nodes appearing every hour. The number of tips increased at about half that rate. In two of the experiments the total recorded volume of the network eventually decreased, and in all cases growth significantly slowed after 24 days. The time-lapse model was only applied while the fungi continued to grow at a rate of at least 0.1 $mm^3 h^{-1}$: a period of 21 days in experiment 1, and 27 days in experiments 2 and 3.

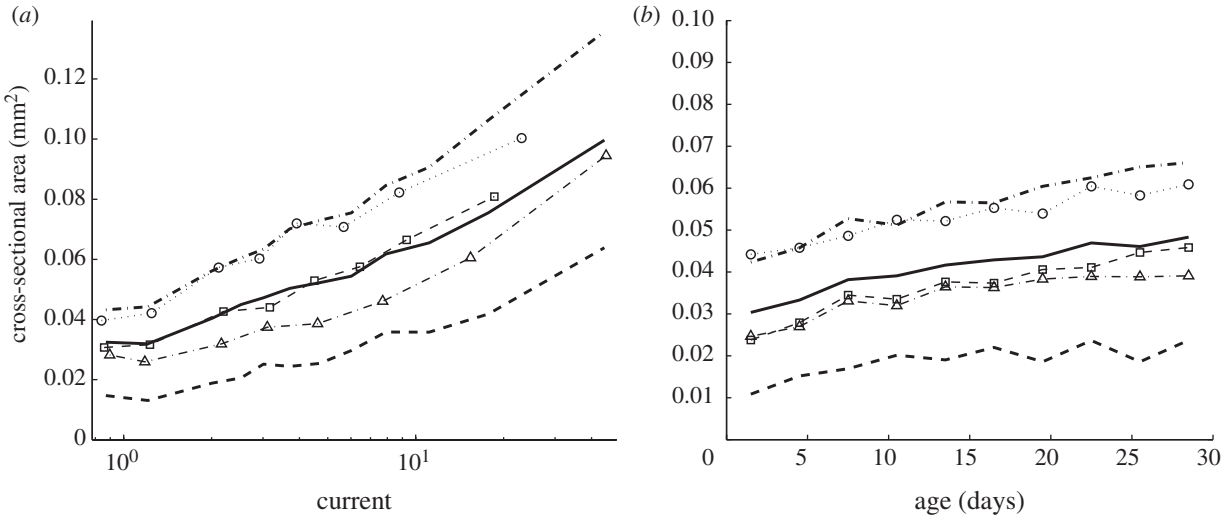

Figure 3. Correlation between cord cross-sectional area and (*a*) the current predicted by the uniform model or (*b*) cord age. Both graphs indicate the mean over all networks (thick solid line), and first and third quartiles over all networks (thick dashed line). Other markers indicate the mean values for individual experiments. (*a*) There was a positive correlation between cross-sectional area and the current in a cord, where current is calculated by applying a unit current to each tip, and we assume constant conductance per unit length. The graph was produced by taking data from all time steps and partitioning it into bins. The first data point marks the mean cross-sectional area for cords with a current of one or less (as was the case for 30% of cords), while the second marks the mean cross-sectional area for cords with a current between one and two (as was the case for 25% of cords). The remaining cords were partitioned into bins of equal size according to the calculated current, and each data point marks the mean current and mean area of one of these bins. (*b*) Although most cords thicken over time, there was only a weak correlation between the age of a cord and its cross-sectional area. Note that the difference in values on the *y*-axis between young and old edges is small compared with the spread within each age group. Current is a better predictor of cross-sectional area.

(a) *Correlation between the cross-sectional area of cords and topological traits*

To assess the relationship between the topological organization of the network and the cross-sectional area of the cords, we used the uniform model, with unit current at each tip and a constant conductance per unit length, to calculate a current for each cord. When using the uniform model, the network at each time point is effectively an independent experiment, and in all cases the calculated currents were correlated with the measured areas. Over the set of all networks, the mean value for the Spearman's rank correlation coefficient between current and cross-sectional area was 0.46 ± 0.09. When we considered the correlation between current and cross-sectional area for the complete set of edges (pooling the data from all the measured networks), the value of ρ was 0.40.

Cords that were closer to the inoculum tended to be thicker, and older edges also tended to be thicker. However, current was a significantly better predictor of area than either distance or age (figure 3). More specifically, over the set of all networks the mean value of ρ between the distance to the inoculum and the cross-sectional area of each cord was -0.37 ± 0.12. When the data from all the networks were pooled, the value of ρ was -0.31. Over the set of all networks (excluding those from the first time step, where, to our knowledge, all edges are the same age) the mean value of ρ between the age and cross-sectional area of the cords was 0.41 ± 0.14. When the data from all the networks were pooled, the value of ρ was 0.21. As the relationship between current and area was reasonably consistent over time and over the three data sets (figure 3), it is possible to use this relationship to predict the size of cords given nothing more than the topology of a fungal network.

(b) *Distribution of currents and speeds*

Both the uniform model and the time-lapse model indicate that many cords carried small currents while a few cords carried much larger currents. Furthermore, the cords that carry exceptionally large currents are sufficiently prevalent to dominate the mean current, so the majority of cords carry a fraction of the mean current. The distribution of predicted speeds was similar, with many small velocities and a few much larger velocities (figure 4). The speeds were calculated using the time-lapse model, with the additional assumption that half the cross-sectional area of each cord was occupied by the interior of the vessels that carry mass flows ($\lambda = 0.5$). Over all time steps and all experiments, 36 per cent of edges carry current at a speed greater than 0.1 $\mu m\ s^{-1}$, 11 per cent of edges carry current at a speed greater than 0.5 $\mu m\ s^{-1}$ and 4 per cent of cords carry current at a speed greater than 1 $\mu m\ s^{-1}$. However, it should be noted that because the imaging process does not capture the growth of fine hyphae, these speeds represent a minimum estimate of the velocity of translocation.

(c) *Correlations between area and the total volume passing through cords*

At each time step the total volume to pass out of each cord was calculated over its history to date. There was a strong, positive correlation between the total volume flowing through a cord and its cross-sectional area (figures 2 and 5). The Spearman's rank correlation coefficient ρ was 0.50, 0.56 or 0.57 in the individual experiments, and $\rho = 0.51$ for the pooled data. The vast majority of cords had a volume between 0.1 and 1 mm^3, and if we select a random edge at a random point in time, there

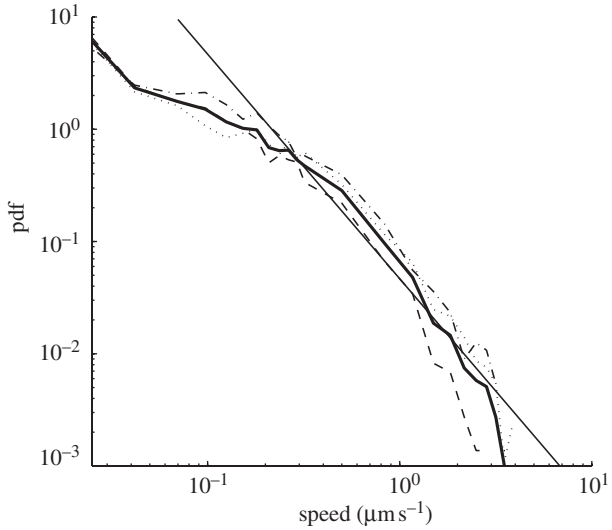

Figure 4. Log–log plot of the probability density function (pdf) of the predicted speed of flow, calculated using the time-lapse model. The thick line indicates the pdf for the pooled data, and the other lines indicate the pdfs for individual experiments. The values for the speeds were calculated with the additional assumption that half the cross-sectional area of each cord was occupied by the interior of the vessels that carry mass flows. For comparison, the straight line represents the pdf for a branching tree of uniform thickness with 2^n 'leaves' carrying mass flows of velocity 0.07 μm s^{-1}, supplied by 2^{n-1} cords carrying mass flows of velocity 0.14 μm s^{-1}, supplied by 2^{n-2} cords carrying mass flows of velocity 0.28 μm s^{-1}, and so on down to a single trunk. The mean speed in such a branching tree would be massively dominated by the few very fast cords. The pdf obtained from the time-lapse model decays more rapidly than a straight line, which indicates that the mean speed in the fungal network is less dominated by the exceptionally large speeds.

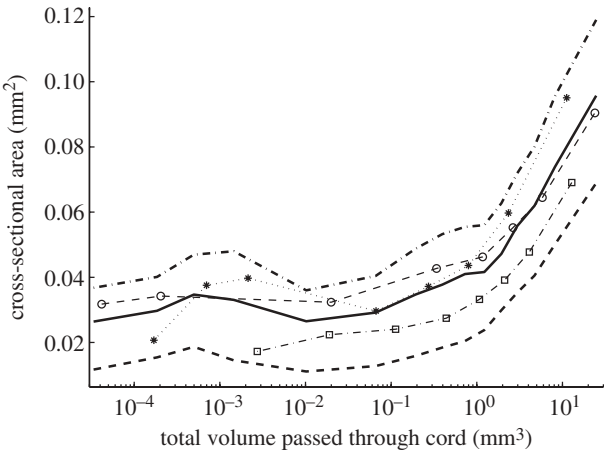

Figure 5. Correlation between cross-sectional area and the total volume to pass through each cord. The data from all experiments and all time steps were partitioned into bins according to the total volume of fluid that had passed through each cord over its history up to each time point. The mean area (thick solid line) and first and third quartile values (thick dashed lines) have been plotted for each bin. The other markers indicate the means for individual experiments.

was a 56 per cent chance that the total volume to leave the cord was greater than the volume of the cord itself.

(d) *Correlations between speed of flow and changes in cross-sectional area*

Cords that were predicted to carry a high velocity current were significantly more likely to increase in size than cords with a low velocity current (figure 6*a*). Spearman's rank correlation coefficient ρ between speed and change in area was 0.34, 0.28 or 0.34 in the individual experiments, and $\rho = 0.33$ for the pooled data. There was also a positive correlation between current and change in cross-sectional area (figure 6*b*), with ρ equal to 0.26, 0.20 or 0.32 in the individual experiments, and $\rho = 0.28$ for the pooled data. Thicker cords tend to carry greater current, but this is to be expected precisely because thicker cords have greater conductance. However, we also found that, given a pair of equally thick cords, the cord that is predicted to carry a greater current is the one that is more likely to thicken (see the electronic supplementary material, §S4 and fig. S2).

5. DISCUSSION

(a) *Growth, water uptake and mass flows are coupled*

If there is growth in a region, there must be a flow of material into that region (see figure 1*b*). When a fungus grows from a central inoculum across an inert substrate (e.g. Tlalka *et al.* 2002, 2003, 2008), any volume for tip growth that is not derived from contracting regions must be acquired by transport from the inoculum. In the microcosms under investigation here, *P. velutina* was allowed to grow over sand that may have absorbed some moisture, so it is possible that water uptake occurred at locations other than the inoculum. However, cords have waxy coatings that insulate them from the environment (Jennings 1987; Rayner *et al.* 1991; Cairney 1992). Our account of growth-induced mass flow indicates an advantage of insulated cords. By reducing the local uptake of water, insulation increases the distance between the sites of water uptake (source) and the regions of growth (sink), thereby increasing the scale of growth-induced mass flows (Banavar *et al.* 1999, 2002; Dreyer & Puzio 2001).

(b) *Transport velocities are determined by the network architecture*

The network architecture will affect the velocity of growth-induced mass flows. At one extreme, consider a binary branching tree where, at every step, every tip branches to produce two offspring, and there is no anastomosis or cord-thickening. At any given moment each generation of cords must carry the same total current out towards the tips, where the speed of flow is equal to the rate of tip growth. It follows that if mothers and daughters have the same cross-sectional area (as is the case for individual hyphae), the velocity of flow in a vessel with n generations of offspring will be 2^n times greater than the rate of tip growth. In principle, this explains how water uptake and growth can induce mass flows at speeds that are orders of magnitude greater than the rate of individual tip growth, and the resulting distribution of velocities is illustrated in figure 4.

At the other extreme, a constant flow rate is predicted in transport systems like the xylem in plants, where

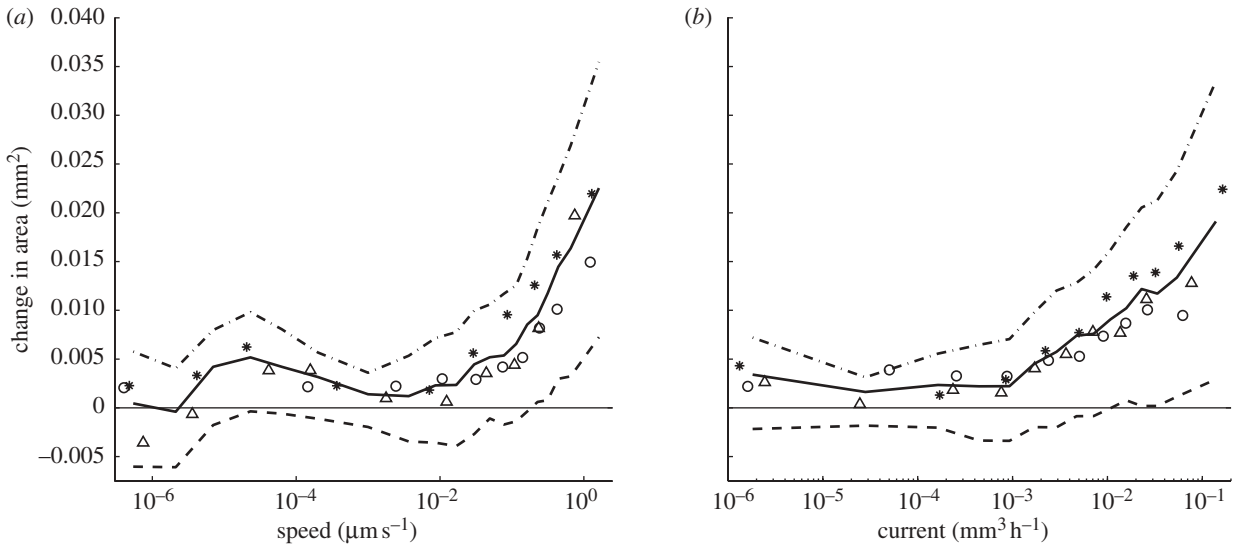

Figure 6. Correlation between the change in cross-sectional area and the predicted flow. The graphs were produced by using the time-lapse model to calculate the current in each cord. The flux density or speed of flow was calculated by assuming that the interior of the vessels carrying the mass flows occupies half the total cross-sectional area. These graphs were produced by partitioning the data from all experiments and all time steps into ten bins of equal size according to the calculated speed or current. Each point on the curve indicates the (*a*) mean speed or (*b*) mean current, plotted against the mean change in cross-sectional area for one of these bins. Thick solid lines indicate the mean over all experiments, and thick dashed lines indicate the first and third quartiles over all experiments. Other markers indicate the mean values for individual experiments.

vascular bundles form a branching hierarchy, but the total cross-sectional area is preserved at every stage (Sherman 1981; Savage *et al.* 2008). Our analysis suggests that the distribution of velocities across the mycelium is closer to the former case (figure 4), with many cords carrying low-velocity mass flows, while some cords carry high-velocity mass flows. However, we cannot yet provide a full quantitative analysis of the predicted velocities as our imaging techniques do not have sufficient resolution to map the fine hyphae that fan out ahead of the developing cords. Thus, the actual volume increase at one of the notional 'tips' characterized here may well be several-fold greater than the volume of the terminal cord that we can measure.

With this caveat, the distribution of predicted currents should reflect the actual currents to the extent that the regions with large amounts of subresolution hyphal growth are also regions where the cords develop and thicken. For example, if we assume that 0.1 mm^3 of fine hyphae grow out of each tip each day, the predicted growth-induced currents would approximately double. This estimate of the volume of fine hyphal growth corresponds to each tip growing a fan of 10 μm thick hyphae, which cover an area of 10 $mm^2\,d^{-1}$. If this coarse estimate of the quantity of fine hyphal growth is accurate, the volume of the digitized cords is only 50 to 60 per cent of the total fungal volume.

To provide a more accurate prediction of the maximum velocities that would be produced if the fluids within fungi simply responded to growth by following the path of least resistance, we would need better morphological information on the number and size of the conducting vessels at each stage of network development. Using the simplifying assumptions that the diameter of the vessel hyphae is constant (12 μm), but the number of conduits scales with the area of the cord and that 50 per cent of the cross-sectional area of the cord comprises conducting vessels, the time-lapse model predicts that 4 per cent of cords carried velocities greater than 1 $\mu m\ s^{-1}$. This 4 per cent of cords that carry the most current approximately corresponds to the major, or most visible, cords in the network.

It may be more realistic to suppose that growth-induced mass flows are carried through vessels that only occupy 10 per cent of the cords' cross-sectional area (rather than the previous estimate of 50%). If we make this assumption, and suppose that 0.1 mm^3 of fine hyphae grows out of each tip each day, our time-lapse model predicts that 4 per cent of cords would carry mass flows with velocity greater than 10 $\mu m\ s^{-1}$. This is comparable with the kinds of velocities observed experimentally in the major cords of *P. velutina*, and greater than those reported for *Schizophyllum commune* (Brownlee & Jennings 1982; Thompson *et al.* 1985, 1987; Connolly & Jellison 1997; Olsson & Gray 1998; Lindahl *et al.* 2001; Tlalka *et al.* 2002). However, as the calculations are critically dependent on the network architecture, estimation of the precise contribution of growth to mass flows would require both detailed volume measurements and very precise velocity measurements on individual microcosms, which is currently beyond our technical capability. Direct comparisons between predicted and measured velocities may be more feasible in the smaller and non-corded networks formed by species such as *Neurospora crassa* (Lew 2005).

(c) *Cords with high current or velocity increase in area*

Mass flows are required to maintain a sufficient supply of nutrients throughout the mycelium, but there are limits to the current that can pass along an individual hypha. High velocities require high pressure gradients, and increasing the velocity of flow means that greater amounts of work must be done by the fungi to overcome viscous drag. Thickening cords and the formation of high-conductivity,

aseptate channels may represent effective responses to these challenges.

We have observed a characteristic relationship between the total current that has passed through a cord and the thickness of that cord (figures 2 and 5). We have also observed a correlation between the currents and the flux densities predicted by our model and the extent to which cords thicken over time (figure 6). Given the further assumption that *P. velutina* has adapted to reduce the work needed to overcome viscous drag, we should expect to see preferential thickening of the high-current cords. This is because, where there is a distribution of currents, significantly greater energy savings can be made by thickening the high-current cords (as opposed to thickening the low-current cords).

There is an element of positive feedback inherent in these observations, as any differential thickening of two parallel transport pathways will automatically increase flow through the cord with greater hydraulic conductivity. However, while we should expect that larger cords will carry greater currents (precisely because they have greater conductance), we have also found that, given a pair of equally thick cords, the cord that is predicted to carry a greater current is the one that is more likely to thicken (see the electronic supplementary material, §S4 and fig. S2).

6. CONCLUSION

In conclusion, we note that the incompressibility of the fluids within fungi ensures that there is a rapid global response to local fluid movements. Furthermore, velocity of fluid flow is a local signal that can convey quasi-global information about the role of a cord within the mycelium. We have found a correlation between the thickening of cords and the speeds or flux densities predicted by our model (figure 6*a* and the electronic supplementary material, fig. S2*a*). Similarly, there was a positive correlation between predicted current and the thickening of cords (figure 6*b* and the electronic supplementary material, fig. S2*b*). This is consistent with the plausible assumption that *P. velutina* has evolved to reduce the work needed to overcome viscous drag, as significantly greater energy savings can be made by preferentially thickening the high-current cords.

The speeds predicted by our model are consistent with experimental data, and the pressure gradients required to produce the predicted flows are very modest (see the electronic supplementary material, §S3). Furthermore, contrary to previous analyses, we suggest that intrahyphal concentration gradients are not strictly necessary for the production of mass flows. The uptake of water and the maintenance of turgor pressure require an osmotic gradient between the hyphae and their environment, but the incompressibility of aqueous fluids ensures that there will be a mass flow from the sites of water uptake to the sites of growth, regardless of the concentration gradients within the mycelium itself. We also suggest that local responses to flux density and nutrient concentration might govern the development of these remarkable self-organizing, efficient, adaptive, growing transport networks.

L.L.M.H. thanks the EPSRC for financial support. N.S.J. thanks the EPSRC and BBSRC. E.L. thanks the EPSRC for grant EP/E056997/1. P.K.M. was partially supported by a Royal Society Wolfson Research Merit Award. M.D.F. thanks the BBSRC and NERC for financial support, and J. Lee for technical assistance.

REFERENCES

Amir, R., Levanon, D., Hadar, Y. & Chet, I. 1995*a* Factors affecting traslocation and sclerotial formation in *Morchella esculenta*. *Exp. Mycol.* **19**, 61–70. (doi:10.1006/emyc.1995.1007).

Amir, R., Steudle, E., Levanon, D., Hadar, Y. & Chet, I. 1995*b* Turgor changes in *Morchella esculenta* during translocation and sclerotial formation. *Exp. Mycol.* **19**, 129–136. (doi:10.1006/emyc.1995.1015).

Banavar, J. R., Maritan, A. & Rinaldo, A. 1999 Size and form in efficient transportation networks. *Nature* **399**, 130–132. (doi:10.1038/20144).

Banavar, J. R., Maritan, A. & Rinaldo, A. 2002 Supply–demand balance and metabolic scaling. *Proc. Natl Acad. Sci. USA* **99**, 10 506–10 509.

Bancal, P. & Soltani, F. 2002 Source–sink partitioning. Do we need Münch? *J. Exp. Bot.* **53**, 1919–1928. (doi:10.1093/jxb/erf037).

Bebber, D., Hynes, J., Darrah, P. R., Boddy, L. & Fricker, M. D. 2007 Biological solutions to transport network design. *Proc. R. Soc. B* **274**, 2307–2315. (doi:10.1098/rspb.2007.0459).

Boddy, L. 1999 Saprotrophic cord-forming fungi: meeting the challenge of heterogeneous environments. *Mycologia* **91**, 13–32. (doi:10.2307/3761190).

Boswell, G., Jacobs, H., Davidson, F. A., Gadd, G. M. & Ritz, K. 2002 Functional consequences of nutrient translocation in mycelial fungi. *J. Theor. Biol.* **217**, 459–477. (doi:10.1006/jtbi.2002.3048).

Boswell, G., Jacobs, H., Davidson, F. A., Gadd, G. M. & Ritz, K. 2003*a* A mathematical approach to studying fungal mycelia. *Mycologist* **17**, 165–171. (doi:10.1017/S0269915X04004033).

Boswell, G., Jacobs, H., Davidson, F. A., Gadd, G. M. & Ritz, K. 2003*b* Growth and function of fungal mycelia in heterogeneous environments. *Bull. Math. Biol.* **65**, 447–477. (doi:10.1016/S0092-8240(03)00003-X).

Boswell, G., Davidson, F. A., Ritz, K., Gadd, G. M. & Jacobs, H. 2007 The development of fungal networks in complex environments. *Bull. Math. Biol.* **69**, 605–634. (doi:10.1007/s11538-005-9056-6).

Brownlee, C. & Jennings, D. H. 1982 Long distance translocation in *Serpula lacrimans*, velocity estimates and the continuous monitoring of induced perturbations. *Trans. Br. Mycol. Soc.* **79**, 43–48.

Cairney, J. W. G. 1992 Translocation of solutes in ectomycorrhizal and saprotrophic rhizomorphs. *Mycol Res.* **96**, 135–141. (doi:10.1016/S0953-7562(09)80928-3).

Clipson, N., Cairney, J. & Jennings, D. 1987 Phosphate uptake by cords and mycelium in the laboratory and the field. *New Phytol.* **105**, 449–457. (doi:10.1111/j.1469-8137.1987.tb00882.x).

Connolly, J. & Jellison, J. 1997 Two-way translocation of cations by the brown rot fungus *Gloeophyllum trabeum*. *Int. Biodeterioration Biodegrad.* **39**, 181–188. (doi:10.1016/S0964-8305(97)00019-X).

Dreyer, O. & Puzio, R. 2001 Allometric scaling in animals and plants. *J Math. Biol.* **43**, 144–156. (doi:10.1007/s002850170001).

Eamus, D. & Jennings, D. 1984 Determination of water, solute and turgor potentials of mycelium of various basidiomycete fungi causing wood decay. *J. Exp. Bot.* **35**, 1782–1786. (doi:10.1093/jxb/35.12.1782).

Eamus, D., Thompson, W., Cairney, J. & Jennings, D. 1985 Internal structure and hydraulic conductivity of

basidiomycete translocating organs. *J. Exp. Bot.* **36**, 1110–1116. (doi:10.1093/jxb/36.7.1110).
Falconer, R. E., Brown, J. L., White, N. A. & Crawford, J. W. 2005 Biomass recycling and the origin of phenotype in fungal mycelia. *Proc. R. Soc. B* **272**, 1727–1734. (doi:10.1098/rspb.2005.3150).
Falconer, R. E., Brown, J. L., White, N. A. & Crawford, J. W. 2007 Biomass recycling: a key to efficient foraging by fungal colonies. *Oikos* **116**, 1558–1568. (doi:10.1111/j.0030-1299.2007.15885.x).
Fricker, M., Boddy, L. & Bebber, D. 2007 Network organisation of mycelial fungi. *The Mycota, vol. VIII: biology of the fungal cell*, pp. 309–330. Berlin, Germany: Springer.
Fricker, M., Lee, J., Bebber, D., Tlalka, M. & Hynes, J. 2008 Imaging complex nutrient dynamics in mycelial networks. *J. Microsc.* **231**, 317–331. (doi:10.1111/j.1365-2818.2008.02043.x).
Gooday, G. W. 1995 The dynamics of hyphal growth. *Mycol. Res.* **99**, 385–394. (doi:10.1016/S0953-7562(09)80634-5).
Gow, N. A. R. & Gadd, G. M. (eds) 1995 *The growing fungus*. London, UK: Chapman and Hall.
Grimmett, G. R. & Kesten, H. 1984 Random electrical networks on complete graphs. *J. Lond. Math. Soc.* **30**, 171–192.
Heath, I. & Steinberg, G. 1999 Mechanisms of hyphal tip growth: tube dwelling amebae revisited. *Fung. Genet. Biol.* **28**, 79–93. (doi:10.1006/fgbi.1999.1168).
Howard, R. 1981 Ultrastructural analysis of hyphal tip cell growth in fungi: Spitzenkörper, cytoskeleton and endomembranes after freeze-substitution. *Cell Sci.* **48**, 89–103.
Jarrett, T., Ashton, D., Fricker, M. & Johnson, N. 2006 Interplay between function and structure in complex networks. *Phys. Rev. Lett. E* **74**, 026116.1–026116.8..
Jennings. 1987 Translocation of solutes in fungi. *Biol. Rev.* **62**, 215–243.
Lew 2005 Mass flow and pressure-driven hyphal extension in *Neurospora crassa*. *Microbiology* **151**, 2685–2692. (doi:10.1099/mic.0.27947-0).
Lew, R., Levina, N., Walker, S. & Garrilll, A. 2004 Turgor regulation in hyphal organisms. *Fung. Genet. Biol.* **41**, 1007–1015. (doi:10.1016/j.fgb.2004.07.007).
Lindahl, B., Finlay, R. & Olsson, S. 2001 Simultaneous, bidirectional translocation of ^{32}P and ^{33}P between wood blocks connected by mycelial cords of *Hypholoma fasciculare*. *New Phytol.* **150**, 189–194. (doi:10.1046/j.1469-8137.2001.00074.x).
López, E., Buldyrev, S. V., Havlin, S. & Stanley, H. E. 2005 Anomalous transport in scale-free networks. *Phys. Rev. Lett.* **94**, 248701.1–248701.4.
Money, N. 1997 Wishful thinking of turgor revisited: the mechanics of fungal growth. *Fung. Genet. Biol.* **21**, 173–187. (doi:10.1006/fgbi.1997.0976).
Money, N. 2008 Insights on the mechanics of hyphal growth. *Fung. Biol. Rev.* **22**, 71–76. (doi:10.1016/j.fbr.2008.05.002).
Nelson, P. 2003 *Biological physics: energy, information, life*, pp. 245–259. New York, NY: W. H. Freeman and Company.
Nobel, P. S. 1991 *Physicochemical and environmental plant physiology*, pp. 473–519. San Diego, CA: Academic Press.
Olsson, S. 2001 Colonial growth of fungi. In *The Mycota, vol. VIII: biology of the fungal cell* (eds R. Howard & N. Gow), pp. 126–141. Berlin, Germany: Springer.
Olsson, S. & Gray, S. N. 1998 Patterns and dynamics of ^{32}P-phosphate and labelled 2-aminoisobutyric acid (^{14}C-AIB) translocation in intact basidiomycete mycelia. *FEMS Microbiol. Ecol.* **26**, 109–120.
Rayner, A. D. M., Watkins, Z. R. & Beeching, J. R. 1991 Self-integration—an emerging concept from the fungal mycelium. In *The fungal colony* (eds N. A. R. Gow, G. D. Robson & G. M. Gadd), pp. 1–24. Cambridge, UK: Cambridge University Press.
Savage, V. M., Deeds, E. J. & Fontana, W. 2008 Sizing up allometric scaling theory. *PLoS Comput. Biol.* **4**, e1000171. (doi:10.1371/journal.pcbi.1000171)
Sherman, T. F. 1981 On connecting large vessels to small: the meaning of Murray's Law. *J. Gen. Physiol.* **78**, 431–453. (doi:10.1085/jgp.78.4.431).
Steinberg, G. 2006 Hyphal growth: a tale of motors, lipids, and the Spitzenkörper. *Eukaryotic Cell* **6**, 351–360. (doi:10.1128/EC.00381-06).
Thompson, W., Eamus, D. & Jennings, D. H. 1985 Water flow through the mycelium of *Serpula lacrimans*. *Trans. Br. Mycol. Soc.* **84**, 601–608. (doi:10.1016/S0007-1536(85)80114-5).
Thompson, W., Brownlee, C., Jennings, D. & Mortimer, A. 1987 Localized, cold-induced inhibition of translocation in mycelia and strands of *Serpula lacrimans*. *J. Exp. Bot.* **38**, 889–899. (doi:10.1093/jxb/38.5.889).
Tlalka, M., Watkinson, S. C., Darrah, P. R. & Fricker, M. D. 2002 Continuous imaging of amino-acid translocation in intact mycelia of *Phanerochaete velutina* reveals rapid, pulsatile fluxes. *New Phytol.* **153**, 173–184. (doi:10.1046/j.0028-646X.2001.00288.x).
Tlalka, M., Hensman, D., Darrah, P. R., Watkinson, S. C. & Fricker, M. D. 2003 Noncircadian oscillations in amino acid transport have complementary profiles in assimilatory and foraging hyphae of *Phanerochaete velutina*. *New Phytol.* **158**, 325–335. (doi:10.1046/j.1469-8137.2003.00737.x).
Tlalka, M., Bebber, D. P., Darrah, P. R., Watkinson, S. C. & Fricker, M. D. 2008 Quantifying dynamic resource allocation illuminates foraging strategy in *Phanerochaete velutina*. *Fung Genet Biol.* **45**, 1111–1121. (doi:10.1016/j.fgb.2008.03.015).
Wells, J. & Boddy, L. 1995 Effect of temperature on wood decay and translocation of soil-derived phosphorus in mycelial cord systems. *New Phytol.* **129**, 289–297. (doi:10.1111/j.1469-8137.1995.tb04299.x).
Wells, J., Boddy, L. & Evans, R. 1995 Carbon translocation in mycelial cord systems of *Phanerochaete velutina*. *New Phytol.* **129**, 467–476. (doi:10.1111/j.1469-8137.1995.tb04317.x).